Investigation of the Differences in the Local Protein Environments Surrounding Tyrosine Radicals $Y_Z^\bullet$ and $Y_D^\bullet$ in Photosystem II Using Wild-Type and the D2-Tyr160Phe Mutant of *Synechocystis* 6803†

Xiao-Song Tang,*,‡ Ming Zheng,§ Dexter A. Chisholm,‡ G. Charles Dismukes,§ and Bruce A. Diner‡

Central Research and Development Department, E. I. du Pont de Nemours & Company, Experimental Station, P.O. Box 80173, Wilmington, Delaware 19880-0173, and Department of Chemistry, Princeton University, Princeton, New Jersey 08544-1009

Received June 30, 1995; Revised Manuscript Received November 22, 1995⊗

ABSTRACT: The reaction center of photosystem II (PSII) of the oxygenic photosynthetic electron transport chain contains two redox-active tyrosines, Tyr160 (Y_D) of the D2 polypeptide and Tyr161 (Y_Z) of the D1 polypeptide, each of which may be oxidized by the primary electron donor, $P680^+$. Spectroscopic characterization of $Y_Z^\bullet$ has been hampered by the simultaneous presence of the much more stable $Y_D^\bullet$, the short lifetime of $Y_Z^\bullet$, and the difficulty in trapping the $Y_Z^\bullet$ radical at low temperature. We present here a method for obtaining an uncontaminated $Y_Z^\bullet$ radical, trapped by freezing under illumination of PSII core complexes isolated from Y_D-less mutants of *Synechocystis* 6803. Specific labeling with deuterium of the β-methylene-3,3- or of the ring 3,5-protons of the PSII reaction center tyrosines in the Y_D-less D2-Tyr160Phe mutant results in a change in the hyperfine structure of the $Y_Z^\bullet$ EPR signal, further confirming that this signal indeed arises from tyrosine. The trapped $Y_Z^\bullet$ radical is also stable for several months at liquid nitrogen temperature. Due to both the absence of contaminating paramagnetic species and the stability at low temperature of $Y_Z^\bullet$, this mutant core complex constitutes an excellent experimental system for the spectroscopic analysis of $Y_Z^\bullet$. We have compared the environments of $Y_Z^\bullet$ and $Y_D^\bullet$ by EPR, ^{1}H ENDOR, and TRIPLE spectroscopies using both mutant and wild-type core complexes, with the following observations: (1) the EPR spectra of $Y_Z^\bullet$ and $Y_D^\bullet$ differ in line shape and line width. (2) Both $Y_Z^\bullet$ and $Y_D^\bullet$ exhibit D_2O-exchangeable ^{1}H hyperfine coupling near 3 MHz, consistent with the presence of a hydrogen bond from a proton donor to the phenolic oxygen atom of a neutral tyrosyl radical. This hyperfine coupling is sharp in the case of $Y_D^\bullet$, indicating the hydrogen bond to be well-defined. In the case of $Y_Z^\bullet$ it is broad, suggestive of a distribution of hydrogen-bonding distances. (3) $Y_D^\bullet$ possesses three additional weak couplings that disappear in D_2O, arising from three or fewer protons (protein or solvent) located within a shell between 4.5 and 8.5 Å. (4) All of the ^{1}H couplings of $Y_D^\bullet$ are sharp, which is indicative of a well-ordered protein environment. (5) All of the ^{1}H couplings in the $Y_Z^\bullet$ spectrum are broad. The environment surrounding $Y_Z^\bullet$ appears to be more disordered and solvent-accessible.

Redox-active tyrosine, Y_Z,[1] of the photosystem II reaction center is oxidized by the primary electron donor, $P680^+$, and then rereduced by the manganese cluster, believed to be the catalytic site of water oxidation [reviewed by Babcock (1987); Debus, 1992; Diner & Babcock, 1996]. Y_Z has been identified by site-directed mutagenesis as tyrosine 161 of the D1 polypeptide (Debus et al., 1988b; Metz et al., 1989). The other redox-active tyrosine, Y_D, of the PSII reaction center has been assigned to tyrosine 160 of the D2 polypeptide by isotopic labeling and site-directed mutagenesis (Barry & Babcock, 1987; Debus et al., 1988a; Vermaas et al., 1988). While its role remains unclear, it has been implicated in a slow oxidation of the S_0 state of the manganese cluster in the dark under special circumstances (Styring & Rutherford, 1987; Vass & Styring, 1991) and may be involved in photoactivation (assembly) of the manganese cluster.

Both $Y_D^\bullet$ and $Y_Z^\bullet$ show similar EPR spectra at room temperature. Small differences in EPR line width have been reported at 77 K on the basis of a comparison of $Y_D^\bullet$ with $Y_Z^\bullet$, trapped upon illumination at 253 K (Mino & Kawamori, 1994). The proton ENDOR spectra were also reported to show similar splittings for the matrix and the 10−20 MHz regions at 20 K, implying similar orientational configurations of the surrounding protons. Nevertheless, $Y_D^\bullet$ and $Y_Z^\bullet$ show very different formation and decay kinetics [for a recent review, see Diner and Babcock (1995)]. Following a light flash, $Y_Z^\bullet$ appears in submicrosecond times in the presence of the manganese cluster (Brettel et al., 1984; Meyer et al., 1989) and in tens of microseconds in its absence (Conjeaud & Mathis, 1980). $Y_D^\bullet$ appears in seconds in both conditions (Babcock & Sauer, 1973; Buser et al., 1992). $Y_Z^\bullet$ decays on the microsecond to millisecond time scale at rates that depend on the oxidation state of the manganese cluster

† This paper is Contribution No. 7195 of the Central Research and Development Department of E. I. du Pont de Nemours & Co. B.A.D. gratefully acknowledges the support of NRI/CRGP of the U.S. Department of Agriculture. Research support at Princeton was provided by NIH-GM39932.

* Address correspondence to this author.

‡ E. I. du Pont de Nemours & Co.

§ Princeton University.

⊗ Abstract published in *Advance ACS Abstracts,* January 15, 1996.

[1] Abbreviations: Chl, chlorophyll *a*; ENDOR, electron nuclear double resonance; EPR, electron paramagnetic resonance; FTIR, Fourier transfer infrared; HEPES, *N*-(2-hydroxyethyl)piperazine-*N*′-2-ethanesulfonic acid; MES, 2-morpholinoethanesulfonic acid; ν_H, proton Larmor frequency; P680, primary electron donor of PSII; PSII, photosystem II; Q_A, primary plastoquinone electron acceptor of PSII; Tris, tris(hydroxymethyl)aminomethane; wt, wild type; Y_D, redox-active tyrosine 160 of the D2 polypeptide; Y_Z, redox-active tyrosine 161 of the D1 polypeptide.

0006-2960/96/0435-1475$12.00/0

(Dekker et al., 1984; Hoganson & Babcock, 1988; van Leeuwen et al., 1993; Rappaport et al., 1994). The fast generation and decay kinetics of $Y_Z^\bullet$ allow PSII photochemistry to occur with high quantum efficiency. $Y_D^\bullet$ decays with multiphasic kinetic components, ranging from seconds to hours (Styring & Rutherford, 1987; Vass & Styring, 1991). In addition to the contrasting rates of reduction, both tyrosines have also been reported to have very different midpoint potentials: approximately 1.0−1.1 and 0.75 V for $Y_Z^\bullet/Y_Z$ and $Y_D^\bullet/Y_D$, respectively (Boussac & Etienne, 1984; Tso et al., 1987; Vass & Styring, 1991; Diner & Babcock, 1996). The high reduction potential of $Y_Z^\bullet/Y_Z$ is essential for PSII activity, as it must be sufficiently oxidizing to drive the oxidation of water.

A detailed spectroscopic analysis of both tyrosines is required to understand what differences in their local protein environments account for their contrasting behaviors. Most of the spectroscopic characterization of the redox-active tyrosines of PSII has concentrated on Y_D. Specific isotopic labeling techniques and ENDOR/ESEEM analysis have allowed a detailed examination of the spin-density distribution in the phenol head group (Barry & Babcock, 1987; Hoganson & Babcock, 1994; Warncke et al., 1994). On the basis of H_2O-/D_2O-exchange data using ENDOR and ESEEM, $Y_D^\bullet$ has been proposed to be a neutral hydrogen-bonded radical (Rodriguez et al., 1987; Barry & Babcock, 1988; Evelo et al., 1989). Computer modeling work has suggested that His190 of the D2 polypeptide (His189 in *Synechocystis*) could both accept the phenol proton upon the oxidation of Y_D and H-bond to the oxidized tyrosyl radical (Svensson et al., 1990; Ruffle et al., 1992). Recently, good experimental support of this view has been obtained by EPR (Tang et al., 1993; Tommos et al., 1993) and ENDOR (Tang et al., 1993) analyses of *Synechocystis* mutants at His189 in the D2 polypeptide.

Compared with the considerable knowledge of Y_D, little is known, however, about the local protein environment and spin-density distribution of $Y_Z^\bullet$, even though physiologically it is the more important. Spectroscopic analysis of $Y_Z^\bullet$ has been limited by two factors: (1) the $Y_Z^\bullet$ radical signal is always overlapped by the signal of $Y_D^\bullet$. In fact, the $Y_Z^\bullet$ signal has only been observed through difference spectra, and as yet no one has been able to observe a clean $Y_Z^\bullet$ signal free of interference from $Y_D^\bullet$. (2) Rapid recombination kinetics at low temperature makes it difficult to trap the $Y_Z^\bullet$ radical, as required for detailed spectroscopic analysis. Recently, Kodera et al. (1992) and Mino and Kawamori (1994) reported that they could trap $Y_Z^\bullet$ at 253 K, followed by cooling to 77 K. However, additional evidence is required to prove that their low-temperature $Y_Z^\bullet$ signal, detected by light minus dark difference spectra, arises exclusively from $Y_Z^\bullet$, particularly in that the reported $Y_Z^\bullet$ and $Y_D^\bullet$ spectra become largely indistinguishable at liquid helium temperature.

Site-directed mutagenesis has made it possible to eliminate Y_D entirely from PSII (Debus et al., 1988a; Vermaas et al., 1988). Ideally, such site-directed mutants should be suitable for $Y_Z^\bullet$ analysis as there is no expected interaction between the two tyrosines. However, Boerner et al. (1993) could not observe a normal EPR spectrum of $Y_Z^\bullet$ in manganese-depleted PSII particles isolated from the D2-Tyr160Phe mutant, despite the fact that the mutant still shows charge recombination kinetics between Q_A^- and $Y_Z^\bullet$ similar to that of wild type. They have suggested that the removal of $Y_D^\bullet$ affects the structure or redox properties of Y_Z.

We present here the first observations of pure $Y_Z^\bullet$ EPR and proton ENDOR spectra trapped by freezing, under illumination, PSII core complexes isolated from a Y_D-less mutant of *Synechocystis* 6803. A specific isotope labeling experiment further confirms that the EPR signal indeed arises from tyrosine. It is clear that loss of Y_D does not affect the structure and properties of Y_Z. We have also carried out an analysis of the decay kinetics for $Y_Z^\bullet$ and estimate the rate constants and activation energies for the decay of $Y_Z^\bullet$. As the $Y_Z^\bullet$ radical is very stable at low temperature and there is no interference of Y_D, this trapping of the normally unstable radical provides us with an excellent experimental system for the spectroscopic analysis of $Y_Z^\bullet$. In this paper, we use PSII core complexes of the Y_D-less mutant and of the wild type to investigate the local protein environments of $Y_Z^\bullet$ and $Y_D^\bullet$ by EPR, proton ENDOR, and proton special TRIPLE spectroscopy. In further collaborations employing this system, we have used saturation−recovery EPR to determine the distances of $Y_Z^\bullet$ and $Y_D^\bullet$ from the non-heme iron of PSII (Koulougliotis et al., 1995), transient proton ENDOR to compare the β-methylene proton hyperfine interactions in $Y_Z^\bullet$ and $Y_D^\bullet$ (Hoganson et al., 1995), and deuterium ESEEM to determine the electron spin-density distribution of the $Y_Z^\bullet$ radical (Tommos et al., 1995).

MATERIALS AND METHODS

Strains and Construction of Mutants. The glucose-tolerant strain of the cyanobacterium *Synechocystis* PCC 6803 (Williams, 1988) was used for all genetic manipulations. The D2-Tyr160Phe and D2-Tyr160Met mutants (D2-tyrosine 160 replaced by phenylalanine and methionine, respectively) were made following a procedure described earlier (Tang et al., 1993) by using the phycocyanin-deficient "olive" strain (Rögner et al., 1990), which has enhanced levels of PSII reaction centers. The presence and integrity of the mutated *psbD*I gene was verified by directly sequencing PCR-amplified DNA in the region of the mutations.

Growth of Cells. Wild-type and D2-Tyr160Phe mutant cells of *Synechocystis* were grown photoheterotrophically at 30 °C under constant illumination for 3−4 days in 18-L carboys in BG-11 (Rippka et al., 1979) containing 5 mM glucose and were bubbled with 5% CO_2 in air. For isotopic labeling experiments, D2-Tyr160Phe mutant cells were grown photoautotrophically in BG-11 medium containing 0.5 mM phenylalanine, 0.25 mM tryptophan, and 0.25 mM deuterated tyrosine for 6−7 days following the method of Barry and Babcock (1987).

Purification of Mn-Depleted PSII Core Complexes. Thylakoid membranes were isolated from wild-type and D2-Tyr160Phe mutant cells according to the procedure described by Rögner et al. (1990), except that buffer A [50 mM HEPES (pH 7.2), 5 mM $CaCl_2$, 5 mM $MgCl_2$, and 25% (w/v) glycerol] was used throughout all steps. The thylakoids were then suspended in buffer B (buffer A plus 15 mM $CaCl_2$), and the chlorophyll concentration was adjusted to 1 mg of Chl/mL. Dodecyl maltoside (1% w/v) was added to extract membrane protein complexes from the thylakoids. After 30 min of gentle stirring in the dark at 4 °C, the sample was centrifuged at 50 000 rpm (Beckman 70 Ti rotor) for 30 min. PSII core complexes were isolated from the supernatant by

using a DEAE-Toyopearl 650s column following the procedure described by Tang and Diner (1994). The eluents with a red absorbance peak equal to or less than 676.5 nm were pooled to maximize PSII recovery and then concentrated by using an Amicon 8400 ultrafiltration cell fitted with a YM-100 membrane. The samples were then subjected to hydroxylapatite column (SynchropakM1HA5-10) chromatography according to the method of Rögner et al. (1990) for complete removal of the manganese cluster from the protein complex and for further purification. The purified PSII core complexes were concentrated by using a Centriprep 100 (Amicon) and desalted by passage through a gel filtration column (Econo-pak 10 DG, Bio-Rad) equilibrated with 50 mM MES−NaOH buffer (pH 6.0) containing 20 mM $CaCl_2$, 5 mM $MgCl_2$, 25% (w/v) glycerol, and 0.03% dodecyl maltoside. For all EPR measurements, the samples were further concentrated to 1 mg of Chl/mL with a Centricon 100 (Amicon), and 0.3 mM potassium ferricyanide was added to the concentrated samples. The PSII core complexes were then loaded into EPR tubes and dark-adapted for 30 min.

Trapping the $Y_Z^\bullet$ Radical at Low Temperature. To trap the rapidly decaying $Y_Z^\bullet$ radical, the core complexes in the EPR tubes were frozen under illumination as follows: the EPR samples were placed at the top (temperature is around 0−4 °C) of an unsilvered dewar half-filled with liquid nitrogen and illuminated with saturating light provided by a tungsten light source (Model I-150, Cuda Products Inc.). During the illumination, the samples were slowly moved toward the liquid nitrogen surface. After 10−20 s, the samples were immersed in liquid nitrogen still under illumination and illuminated a few more seconds, and then the light was turned off. The samples were stored in liquid nitrogen until use.

EPR, ENDOR, and Special TRIPLE. EPR spectra were recorded at 150 K by using an Oxford ESR-910 helium flow cryostat on a Bruker ER200D spectrometer equipped with an upgraded computer software system (ESP-300 Model). ENDOR and special TRIPLE spectra were recorded by using a Bruker ESP300/ER250A EPR/ENDOR spectrometer operating with a Bruker cavity and Bruker r.f. helix/dewar resonating in the TM_{110} mode. All measurements were performed at 120−135 K using a liquid nitrogen flow system (Bruker, variable-temperature unit, ER4111VT).

H_2O/D_2O Exchange. For the H_2O-/D_2O-exchange experiments, PSII core complexes were suspended in a buffer containing 20 mM HEPES−NaOH (pH or pD 7.5), 0.03% dodecyl maltoside, and 10 mM NaCl prepared in either H_2O or D_2O, followed by a 14−16-h incubation at 4 °C in the dark.

RESULTS

The purity and properties of the PSII core complex purified by the procedure described in the Materials and Methods section are very similar to those of a PSII preparation described by Rögner et al. (1990), but with somewhat higher specific activity (38 Chl per photoreducible Q_A as opposed to 45−48). The PSII complexes prepared from the wild-type and D_2-Tyr160Phe mutants by the current procedure are completely inactive in oxygen evolution. There is also no manganese associated with the complex, which is capable of reducing $Y_Z^\bullet$. These PSII preparations could, therefore, be used to directly observe the long-lived $Y_Z^\bullet$ radical signal without any further treatment to remove the Mn cluster. At room temperature, a $Y_Z^\bullet$ EPR signal, with a spin concentration at a 1:1 ratio compared with $Y_D^\bullet$, is observed in the wild-type PSII complex under continuous illumination with saturating light (data not shown), as reported by Metz et al. (1989).

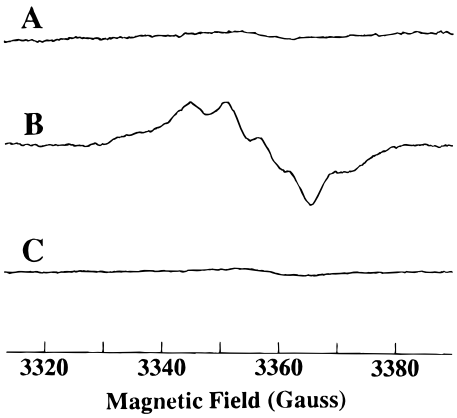

FIGURE 1: EPR spectra of a PSII core complex isolated from the *Synechocystis* 6803 D2-Tyr160Phe mutant. The EPR samples were prepared as follows: (A) dark-adapted; (B) frozen under illumination; and (C) thawed and refrozen in the dark. For further details, see the text. Instrument settings: modulation frequency, 100 kHz; microwave frequency, 9.46 GHz; modulation amplitude, 2 G; microwave power, 0.1 mW; temperature, 150 K.

The mutant PSII core complex shows practically no EPR signal in the $g = 2$ region in a dark-adapted sample. The residual signal corresponds to less than 0.01 spin per reaction center of an 8−10 G narrow radical signal, probably arising from trace PSI contamination (Figure 1A). The $Y_Z^\bullet$ radical can be trapped by freezing the PSII sample under illumination in the presence of ferricyanide, as described in the Materials and Methods section. Figure 1B shows the low-temperature $Y_Z^\bullet$ EPR spectrum observed in the PSII core complex of the D2-Tyr160Phe mutant. The trapped $Y_Z^\bullet$ radical completely disappears in less than 5 s upon thawing (Figure 1C). Compared with the EPR spectrum of the dark-adapted sample (Figure 1A), the spectrum after trapping under illumination and thawing (Figure 1C) shows little increase, indicating the reversibility of radical generation and decay.

The $Y_Z^\bullet$ radical, trapped in the D2-Tyr160Phe mutant, is very stable at low temperature and can be stored at 77 K for months with no loss of amplitude. While stable during the time course of the measurement of Figure 1, it is unstable upon warming above 150 K. Further details on its lifetime as a function of temperature are shown in Figure 2. In this experiment, the sample was incubated for 30 s at each of the indicated temperatures. Half of the $Y_Z^\bullet$ signal is lost upon a 30-s incubation at 252 K. There is virtually no Q_A^- trapped under the conditions that trap $Y_Z^\bullet$, and the source of reductant for the reduction of $Y_Z^\bullet$ upon warming is ferrocyanide.

The experimental conditions that result in the trapping of $Y_Z^\bullet$ in the mutant and wild type give rise to nearly 1 spin of $Y_Z^\bullet$ radical per reaction center, using $Y_D^\bullet$ of wild type as a spin standard. The spectrum of $Y_Z^\bullet$ in the D2-Tyr160Phe mutant is similar to the well-known, normal $Y_Z^\bullet$ EPR spectrum obtained from wild-type *Synechocystis* or higher plant samples at room temperature (Babcock & Sauer, 1975; Hoganson & Babcock, 1988; Metz et al., 1989). A similar

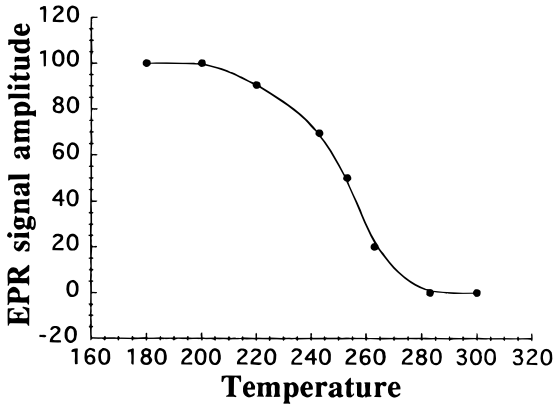

FIGURE 2: Stability of the $Y_Z^\bullet$ EPR signal at various temperatures. The $Y_Z^\bullet$ radical was first trapped as described in the Materials and Methods section, and the EPR amplitude measured at 150 K was taken as a 100% reference. The sample was then incubated at the indicated temperature for 30 s in an ethanol or acetone−dry ice bath, followed by the measurement of the $Y_Z^\bullet$ EPR signal once more at 150 K. The sample was then quickly thawed, and the preceding experiment was repeated for another incubation temperature. Instrument settings were the same as for Figure 1.

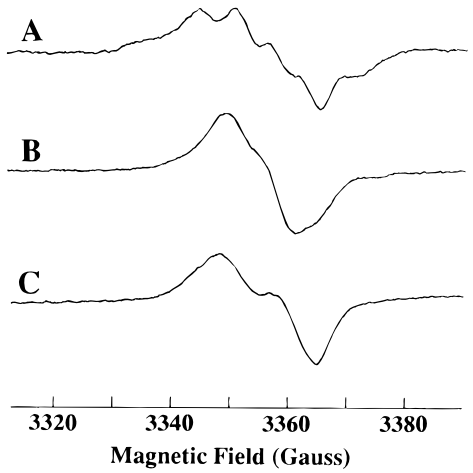

FIGURE 3: Light-induced $Y_Z^\bullet$ EPR spectra of PSII core complexes purified from the D2-Tyr160Phe mutant cells grown on normal BG-11 medium (A) or in the presence of the β-methylene-3,3-deuterated tyrosine (B) or the ring-3,5-deuterated tyrosine (C). For further details, see Materials and Methods. Instrument settings were the same as for Figure 1.

result has also been obtained for the PSII core complex isolated from the D2-Tyr160Met mutant (data not shown).

To further confirm that the light-induced EPR signal in the D2-Tyr160Phe mutant indeed arises from a tyrosine residue, an experiment was carried out in which tyrosine was specifically labeled. By growing the D2-Tyr160Phe mutant cells under conditions of functional aromatic amino acid auxotrophy [see Materials and Methods and Barry and Babcock (1987)], we were able to deuterate the β-methylene-3,3- (Figure 3B) or the ring 3,5-positions (Figure 3C) of the phenolic ring of the reaction center tyrosine in this mutant. In this numbering system, the OH group is bound at C4. A spectrum of the light-induced EPR signal of the PSII core complexes isolated from these cells (Figure 3B,C) shows a change in the hyperfine structure compared to that of the same mutant grown in normal BG-11 medium (Figure 3A). The EPR spectra, observed here using the deuterated samples, are similar to those observed in deuterated model tyrosine radicals (Barry et al., 1990). These results clearly demonstrate that the light-induced EPR signal, trapped at low

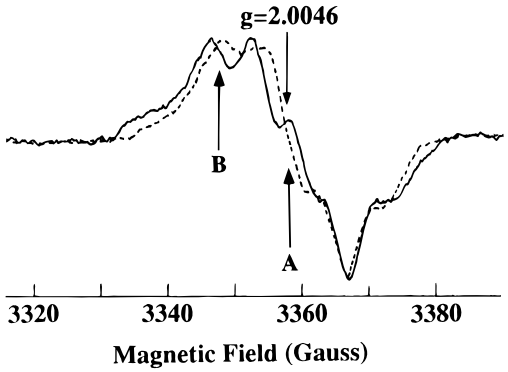

FIGURE 4: Comparison of the EPR spectra of the dark-stable $Y_D^\bullet$ radical (broken line) generated in a wild-type PSII core complex and the light-induced $Y_Z^\bullet$ radical (solid line) generated in a PSII core complex from the D2-Tyr160Phe mutant. Instrument settings were the same as for Figure 1.

temperature in the D2-Tyr160Phe mutant, indeed arises from tyrosine. A similar change in the hyperfine structure of tyrosine, accompanying deuteration, has been previously reported for the $Y_D^\bullet$ radical in wild type (Barry & Babcock, 1987) and in the D2-His189Gln mutant (Tang et al., 1993), as well as for $Y_Z^\bullet$ at room temperature in wild type (Boerner & Barry, 1993). These results are consistent with a concentration of spin density at the C1, C3, and C5 positions, as in the case of $Y_D^\bullet$ [see also Tommos et al. (1995)]. We also conclude from these results that the removal of Y_D does not affect the structure and properties of the $Y_Z^\bullet$ radical in the PSII reaction center, in contrast to what has been reported previously (Boerner et al., 1993).

Figure 4 compares the EPR spectra of $Y_D^\bullet$ and $Y_Z^\bullet$ in PSII core complexes isolated from the wild-type and D2-Tyr160Phe mutants, respectively, measured with a 2-G modulation amplitude and 0.1 mW of microwave power at 150 K. No further hyperfine structural features could be resolved for either EPR signal by using modulation amplitudes of less than 2 G. However, slightly higher modulation amplitudes (3 or 4 G) reduce the resolution of the $Y_Z^\bullet$ spectrum, but have no effect on the $Y_D^\bullet$ spectrum (data not shown). By comparing what is the best-resolved EPR spectrum of $Y_Z^\bullet$ with that of $Y_D^\bullet$, we have found the following differences: (1) a new peak is observed in the center of the $Y_Z^\bullet$ spectrum that is absent from the $Y_D^\bullet$ spectrum. This peak is too narrow to be coming from contaminating radicals, either chlorophyll cation radicals or Fe-uncoupled Q_A^-. (2) The line width of $Y_Z^\bullet$ is 2−3 G wider than that of $Y_D^\bullet$, in agreement with Mino and Kawamori (1994). These results suggest that the local protein environments differ around each of the two redox-active tyrosines.

The microwave power dependence of the amplitudes of $Y_Z^\bullet$ and $Y_D^\bullet$ provides information on the relaxation properties of the radicals and can be used to detect the presence of dipolar interactions with other paramagnetic centers. This dependence was examined at three different temperatures (Figure 5). Differences in the microwave power saturation of $Y_Z^\bullet$ and $Y_D^\bullet$ in the presence of the manganese cluster have been interpreted as indicating a closer proximity of $Y_Z^\bullet$ than $Y_D^\bullet$ to the cluster (Warden et al., 1976; Babcock et al., 1989). In the absence of the manganese cluster, however, the EPR signals of $Y_Z^\bullet$ and $Y_D^\bullet$ measured at 100-kHz modulation frequency show very similar saturation curves over the temperature range from 10 to 140 K. The $P_{1/2}$ was estimated

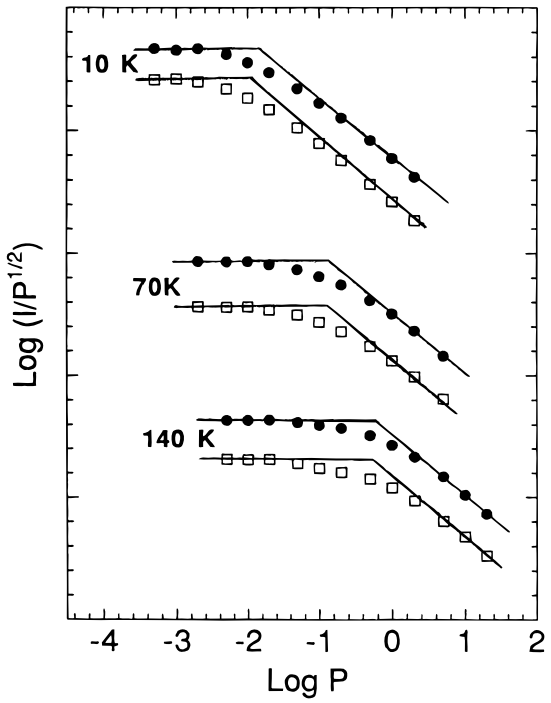

FIGURE 5: Microwave power saturation curves of the EPR signals of the dark-stable $Y_D^\bullet$ radical in a wild-type PSII core complex (closed circles) and the light-induced $Y_Z^\bullet$ radical in a D2-Tyr160Phe PSII core complex (open squares) at three different temperatures. Experimental conditions are the same as in Figure 1, except for the microwave power. The curves have been displaced vertically for clarity and are not intended to show the absolute signal amplitudes.

to be 0.015, 0.15, and 0.6 mW at 10, 70, and 140 K, respectively. The results obtained from Figure 4 and those obtained by Koulougliotis et al. (1995) show that, in the absence of the manganese cluster, the $Y_Z^\bullet$ and $Y_D^\bullet$ radicals have similar T_1 relaxation properties, accelerated only by the non-heme iron.

Figure 6 shows ^{1}H ENDOR spectra in the matrix region ($\nu_H \pm 2.2$ MHz) for both the dark-stable $Y_D^\bullet$ and the photogenerated $Y_Z^\bullet$ radicals measured at 120 K in PSII core complexes isolated from wild-type and D2-Tyr160Phe mutant cells, respectively. ENDOR spectra were recorded at the two EPR resonance positions noted in Figure 4 and found to be essentially the same. Difference spectra ($H_2O - D_2O$) were identical at both EPR resonance positions. The matrix ^{1}H ENDOR spectra of $Y_Z^\bullet$ and $Y_D^\bullet$ are quite different; $Y_D^\bullet$ has more resolved peaks with narrower line widths than $Y_Z^\bullet$. This region predominantly corresponds to the distant dipolar coupled protons. There is no clear correspondence between peaks found in $Y_D^\bullet$ and those in $Y_Z^\bullet$, indicating different microenvironments for the two radicals. For easy comparison, all of the ^{1}H hyperfine couplings are listed in Table 1.

Upon incubation in D_2O for 14−16 h at pH = pD = 7.5, couplings with strengths 0.13 (A_dA_d'), 0.66 (D_dD_d'), 0.91 (E_dE_d', weak), and 1.30 MHz (G_dG_d') in the $Y_D^\bullet$ spectra (Figure 6a−c) are decreased in intensity. The difference between the two $Y_D^\bullet$ spectra, after normalization against the integrated EPR intensity, is shown directly in Figure 6c. The same D_2O-exchange treatment on the $Y_Z^\bullet$ sample leads to a quite different spectral change; peaks labeled A_zA_z' and B_zB_z' actually gain intensity after exchange (Figure 6d,e). This is seen by the reversed phase in the difference spectrum given in Figure 6f, after normalization against the integrated EPR intensity. Intensification of ^{1}H ENDOR peaks can occur when spin diffusion of magnetization is decreased upon D_2O exchange (see Discussion).

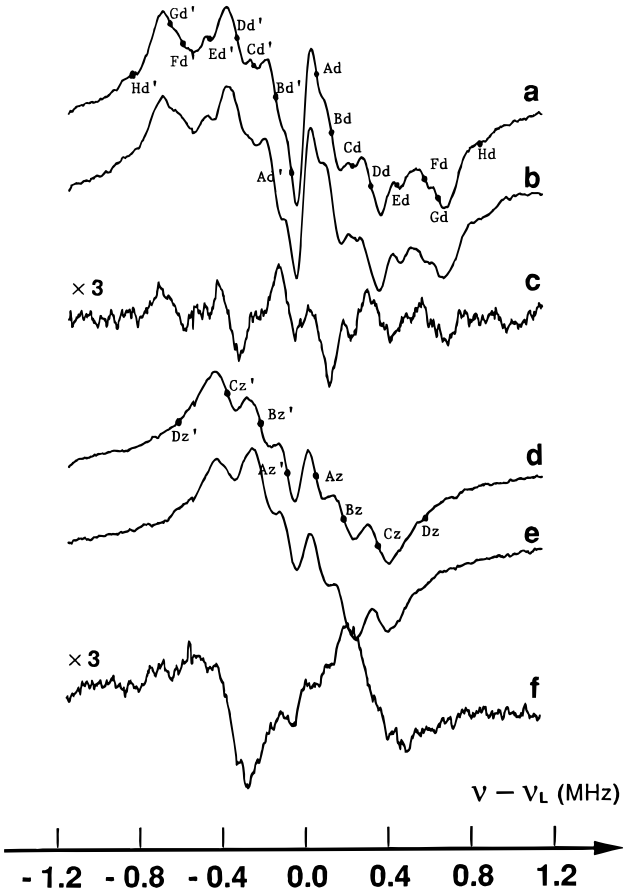

FIGURE 6: ^{1}H ENDOR spectra of $Y_D^\bullet$ and $Y_Z^\bullet$ radicals from wild-type and D2-Tyr160Phe mutant PSII core complexes incubated for 14−16 h in H_2O or D_2O buffer: (a) $Y_D^\bullet$ with H_2O buffer; (b) $Y_D^\bullet$ with D_2O; (c) (a) − (b); (d) $Y_Z^\bullet$ with H_2O buffer; (e) $Y_Z^\bullet$ with D_2O buffer; (f) (d) − (e). Instrument conditions: rf modulation frequency, 12.5 kHz; rf modulation depth, 100 kHz; rf power, 50 W; microwave power, 1 mW; temperature, 120 K.

Table 1: ^{1}H Hyperfine Couplings (MHz) in the $Y_D^\bullet$ and $Y_Z^\bullet$ ENDOR Spectra

$Y_D^\bullet$		$Y_Z^\bullet$		D_2O exchangeability[a]
A_dA_d'	0.13			e
		A_zA_z'	0.14	st
B_dB_d'	0.27			ne
		B_zB_z'	0.40	st
C_dC_d'	0.48			ne
D_dD_d'	0.66			e
		C_zC_z'	0.75	ne
E_dE_d'	0.91			e
		D_zD_z'	1.12	ne
F_dF_d'	1.17			ne
G_dG_d'	1.30			e
H_dH_d'	1.68			ne
I_dI_d'	2.7	E_zE_z'	3.1	e
		F_zF_z'	3.61	ne
J_dJ_d'	4.22			ne
K_dK_d'	4.78			ne
		G_zG_z'	5.20	ne
L_dL_d'	7.00			ne
		H_zH_z'	7.30	ne
M_dM_d'	7.33			ne

[a] e, exchangeable; ne, nonexchangeable; st, stimulated.

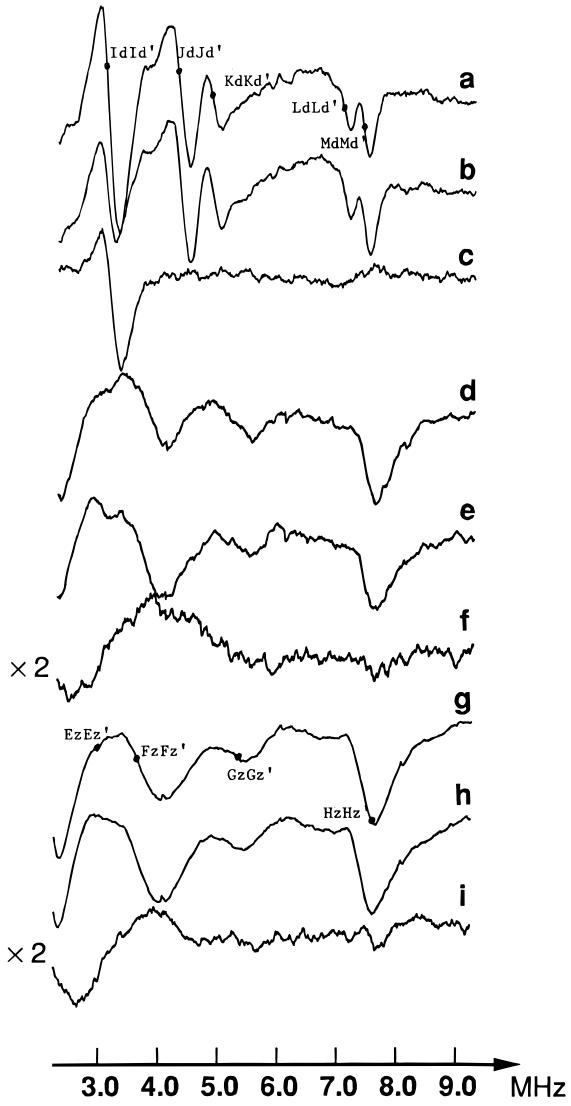

FIGURE 7: ^{1}H special TRIPLE spectra of $Y_D^\bullet$ and $Y_Z^\bullet$ radicals from wild-type and D2-Tyr160Phe mutant PSII core complexes incubated for 14−16 h in H_2O or D_2O buffer: (a) $Y_D^\bullet$ with H_2O buffer; (b) $Y_D^\bullet$ with D_2O; (c) (a) − (b); (d and g) $Y_Z^\bullet$ with H_2O buffer; (e and h) $Y_Z^\bullet$ with D_2O buffer; (f) (d) − (e); (i) (g) − (h). Instrument conditions: rf modulation frequency, 25 kHz for a−f and 50 kHz for g−i; rf modulation depth, 100 kHz for a−f and 200 kHz for g−i; microwave power, 4 mW. rf power settings: attenuator A1, 11 dB; A2, 5 dB; A3, 0 dB down from 50 W, respectively. Temperature was 135 K. The frequency axis has been converted to hyperfine frequency.

Outside the matrix region, ^{1}H couplings in both $Y_D^\bullet$ and $Y_Z^\bullet$ were measured using the special TRIPLE mode to take advantage of the 2-fold higher sensitivity and spectral resolution. The results are shown in Figure 7 and listed in Table 1. The $Y_D^\bullet$ spectra were recorded at a radio frequency modulation depth of 100 kHz, while those of $Y_Z^\bullet$ were recorded at 100 and 200 kHz. The 200-kHz spectra are also shown for $Y_Z^\bullet$ because of the better signal/noise ratio compared to the 100-kHz spectra in the lower concentration $Y_Z^\bullet$ sample.

The $Y_D^\bullet$ spectra (Figure 7a,b) again show much narrower line widths and more resolved peaks than the $Y_Z^\bullet$ spectra (Figure 7d,e,g,h). D_2O exchange in the $Y_D^\bullet$ sample leads to a more than 50% reduction in intensity of the coupling I_dI_d' at 3.1 MHz, as seen in the difference spectrum (Figure 7c). We define here the characteristic frequency of the I_dI_d' transition as the zero-crossing point of the derivative signal at 3.1 MHz, while in Tang et al. (1993) the negative peak position of the derivative signal was used and given as 3.5 MHz. Figure 7c reveals a narrow line shape for the exchangeable proton that is typical of the perpendicular component of an axial hyperfine tensor with a peak-to-peak line width of 0.3 MHz. This result is consistent with the previous ^{1}H ENDOR work on $Y_D^\bullet$. The line shape, in particular, is in accordance with the exchangeable proton previously assigned to a hydrogen bond to the phenolic oxygen, which predominantly interacts through a dipolar coupling mechanism (Rodriguez et al., 1987; Evelo et al., 1989; Tang et al., 1993). This narrow single peak in the $Y_D^\bullet$ spectra is replaced by a considerably broader and weaker peak between 2.2 and 3.2 MHz in the $Y_Z^\bullet$ spectra, as shown in Figure 7f,i. This broad feature probably arises from a distribution of hydrogen bonds to $Y_Z^\bullet$, as will be discussed in the next section. Those components that do not show D_2O/H_2O exchange originate from the ring and β-methylene protons of $Y_Z^\bullet$, as determined by deuterium ESEEM (Tommos et al., 1995).

The $Y_D^\bullet$ and $Y_Z^\bullet$ spectra in both the matrix region (Figure 6) and in the 2−9-MHz range of hyperfine frequencies (Figure 7), recorded in the presence of H_2O and D_2O, are highly reproducible, as indicated by measurements on three independent sets of samples. The signal amplitudes in cw ENDOR depend on electron nuclear relaxation processes that are not necessarily identical in H_2O and D_2O. Such differences, should they exist, would be expected to be still smaller using the TRIPLE mode (Figure 7). However, while one might quibble with the EPR-based normalization used for the difference spectra of Figures 6c,f and 7c,f,i, the same treatment of the data was used for both $Y_D^\bullet$ and $Y_Z^\bullet$. The very different results for the H_2O-D_2O difference spectra of $Y_D^\bullet$ and $Y_Z^\bullet$ indicate that the environments in which each of them are located are really not at all the same. Furthermore, the axial line shape obtained for the exchangeable proton in the case of $Y_D^\bullet$ (Figure 7c) is fully consistent with what one would expect for the perpendicular component of an axial hyperfine tensor arising from a purely dipolar coupled proton.

DISCUSSION

Directed mutagenesis, isotopic labeling, and spectroscopic techniques have provided a deeper understanding of the local protein environment, spin-density distribution, and localization of $Y_D^\bullet$. Through this paper and associated publications (Koulougliotis et al., 1995; Hoganson et al., 1995; Tommos et al., 1995), we are attempting to perform a similar in-depth analysis of $Y_Z^\bullet$. Such information should help us to understand the differences in the local protein environments of $Y_Z^\bullet$ and $Y_D^\bullet$ and to account for the functional differences between these two redox-active tyrosines. Until now, detailed spectroscopic characterization of $Y_Z^\bullet$ has been limited by interference from $Y_D^\bullet$ and the difficulty in trapping $Y_Z^\bullet$ at low temperature. The present paper describes an experimental system that enables us to avoid these problems entirely. As shown here and in Tommos et al. (1995), we can use this experimental system for probing the protein environment and for assigning the spin density of $Y_Z^\bullet$. Moreover, by using this system and the technique of saturation−recovery EPR spectroscopy, we have been able to show that $Y_Z^\bullet$ and $Y_D^\bullet$ are equidistant from the non-heme iron of PSII (Koulougliotis et al., 1995). This result provides

direct experimental evidence in support of bilateral symmetry in the reaction center of photosystem II, with regard to the locations of $Y_Z^\bullet$ and $Y_D^\bullet$, and further support for their assignments to D1-Tyr161 and D2-Tyr160, respectively.

A new non-oxygen-evolving PSII core complex preparation derived from Rögner et al. (1990) and Tang and Diner (1994) was used for the current experiments. This procedure avoids the overnight sucrose-density-gradient centrifugation, used in the preparation of Rögner et al. (1990), and the high-concentration Tris wash, used by Boerner et al. (1993). This preparation has the dual advantage of involving a simple procedure for isolating highly purified PSII core complexes and being sufficiently gentle to produce PSII core complexes with high levels of photoactivity.

A number of spectroscopic methods have been used to probe for environmental factors that influence the kinetics of oxidation and the redox properties of $Y_Z^\bullet$ and $Y_D^\bullet$ [see Barry (1993), Hoganson and Babcock (1994), and Diner and Babcock (1996) for recent reviews]. These include the use of EPR to probe for differences in the sensitivity of $Y_Z^\bullet$ and $Y_D^\bullet$ to site-directed mutations, to examine their ability to broaden the EPR signal of $P680^+$, and to measure their power saturation characteristics as a function of S state, the use of ENDOR to examine the temperature dependence of line widths of weakly coupled matrix protons, and the use of FTIR to examine subtle differences in vibrational spectra and the consequences of site-directed mutations and/or D_2O/H_2O exchange.

EPR. The two traditional sources of contamination of the $Y_Z^\bullet$ magnetic resonance spectra have been $Y_D^\bullet$ and a 7−10-G narrow radical (possibly a Chl cation) in manganese-depleted PSII core complexes. There is no $Y_D^\bullet$ radical in the D2-Tyr160Phe mutant core complex, and we are able to generate and trap the $Y_Z^\bullet$ radical under conditions (short illumination time, 10−20 s; low temperature, 0−4 °C) that are sufficiently mild to preclude the generation of the 7−10-G narrow radical. Consequently, we present here the first "clean" $Y_Z^\bullet$ EPR spectrum, uncontaminated by $Y_D^\bullet$. A comparison of the EPR spectra of $Y_Z^\bullet$ and $Y_D^\bullet$ (Figure 4) shows clear differences in line shapes and line widths. A narrow feature at the center of the EPR spectrum of $Y_Z^\bullet$ could be misconstrued as being caused by the presence of a new paramagnetic species other than tyrosine, the signal from which superimposes itself upon the normal tyrosine $Y_Z^\bullet$ signal. However, the tyrosine deuteration experiment (Figure 3) argues against this possibility, as does its extremely narrow line width and its reproducibility from sample to sample. The fact that the feature disappears in the β-methylene-3,3-deuterated tyrosine samples (Figure 3B) demonstrates that it is indeed part of the tyrosine signal. Furthermore, Hoganson and Babcock (1988) have reported a flash-induced, room-temperature, transient $Y_Z^\bullet$ spectrum in Tris-washed PSII membranes that shows evidence of the central feature that we report in the trapped radical (Figure 4). A further control experiment was performed in which a sample containing trapped $Y_Z^\bullet$ was warmed to 250 K for 30 s, which decreases the signal amplitude by one-half (see Figure 2). The remaining signal gave the same line shape as initially generated, indicating that the narrow feature is an integral part of the $Y_Z^\bullet$ EPR spectrum.

It has been reported by Boerner et al. (1993) that the mutation D2-Tyr160Phe affects the structure and redox properties of $Y_Z^\bullet$. However, the localization of Y_Z and Y_D in different polypeptides, the ability of the D2-Tyr160Phe mutant to grow photoautotrophically (Debus et al., 1988a; Vermaas et al., 1988), the observation of a normal S_2 state multiline signal (Kirilovsky et al., 1992) in this mutant, the measurement of similar kinetics of charge recombination between Q_A^- and oxidized Y_Z (Boerner et al., 1993) in mutant and wild type, and finally the observation presented here of an EPR spectrum for $Y_Z^\bullet$ in this mutant similar to that observed in an unfrozen wild-type sample (Hoganson & Babcock, 1988) all argue that the properties of $Y_Z^\bullet$ in the mutant are similar, if not identical, to those in wild type. The reason for the alteration of the $Y_Z^\bullet$ EPR spectrum in the earlier study of the D2-Tyr160Phe mutant (Boerner et al., 1993) remains unclear.

ENDOR. For protons lacking scalar couplings, i.e., those that are not part of the covalent structure of the radical, magnetic dipolar coupling yields ENDOR peaks in the matrix region approximately $\nu_H \pm 1$ MHz, i.e., from protons located between 3.5 and 8.5 Å from a point center of electron spin density. Thus, the matrix ENDOR region gives a fingerprint of the magnetic microenvironment of the paramagnetic center under investigation. The difference seen in both the matrix ^1H ENDOR spectra (Figure 6a,d) and the deuteron exchange profiles (Figure 6c,f) of $Y_D^\bullet$ and $Y_Z^\bullet$ clearly indicate that they have very different microenvironments. For $Y_D^\bullet$, there are 3−4 pairs of couplings that are decreased in intensity upon D_2O exchange, most probably due to 3−4 or possibly fewer exchangeable protons in the range 0.13−1.3 MHz and suggestive of distances in the range 3.9−8.5 Å, by using the point dipole approximation. These exchangeable protons are most likely associated with protein residues or possibly a few ordered water molecules.

For $Y_Z^\bullet$, however, D_2O exchange appears to increase the intensity of the matrix peaks A_zA_z' and B_zB_z'. The origin of the enhancement effect probably originates in a decrease in the spin diffusion of magnetization from the detected (i.e., nonexchangeable) protons to nearby solvent protons [for theory, see Meier (1994)]. This nuclear spin-relaxation pathway would be reduced when deuterons replace protons in the solvent, due to their weaker magnetic moments (by a factor of 3.3) and their different resonance frequencies. Since, in a proton-rich protein environment, H_2O/D_2O exchange at only a few sites is unlikely to block the spin-diffusion process (Wu et al., 1989), there are likely to be multiple exchangeable protons, most likely bulk solvent water molecules, near to the A_zA_z' and B_zB_z' protons. The result is a stronger proton ENDOR intensity when dipolar coupling to protons is replaced by deuterons. The exchangeable protons that produce this effect need not be directly observable in the ENDOR spectrum, either because they are disordered or too far away.

$Y_D^\bullet$ has been proposed to be a hydrogen-bonded neutral (deprotonated) tyrosine free radical in which the phenolic oxygen is hydrogen-bonded by a nearby protonated base (e.g., histidine) (Rodriguez et al., 1987; Babcock et al., 1989; Evelo et al., 1990; Svensson et al., 1990). Figure 7c shows that there is an exchangeable proton with a narrow axial line shape at 3.1 MHz, characteristic of dipolar coupling. By using a point dipole approximation and a spin density of 0.25 on the phenolic oxygen (Tommos et al,. 1995), one can calculate an oxygen−hydrogen distance of 1.85 Å, consistent only with a well-ordered hydrogen bond. Recent experimental evidence from site-directed mutagenesis and EPR and

ENDOR spectroscopy has been presented that supports this hypothesis, in particular pointing to D2-His189 either hydrogen-bonding directly to $Y_D^\bullet$ (Tang et al., 1993; Tommos et al., 1993) or through a water molecule or other residue. The next closest exchangeable proton to $Y_D^\bullet$ is the one at 1.3 MHz, which at 2.48 Å is at best a weak hydrogen bond. With the exception of three or four exchangeable proton sites, $Y_D^\bullet$ is likely located in a largely apolar, well-ordered environment, distant from bulk solvent water.

On the other hand, the observation of ENDOR enhancement of $Y_Z^\bullet$ in PSII particles depleted of the tetramanganese cluster (Figure 6f) probably indicates that solvent water molecules are more accessible to a site near to $Y_Z^\bullet$ than to $Y_D^\bullet$. These water molecules are likely to be located at or near the site of manganese coordination. This accessibility and distance are consistent with molecular modeling of the PSII structure (Svensson et al., 1990, 1991; Ruffle et al., 1992) and with the observation that $Y_Z^\bullet$ is more accessible to exogenous reductants than $Y_D^\bullet$ (Yerkes & Babcock, 1980). The functioning of $Y_Z^\bullet$ in the water-oxidizing complex as a direct catalyst for substrate activation (Gilchrist et al., 1995; Hoganson et al., 1995; Tommos et al., 1995) would be structurally consistent with these results.

In the TRIPLE H_2O-D_2O difference spectrum of $Y_Z^\bullet$ (Figure 7f,i), we see a broad negative transition at around 2.7 MHz, which is quite unlike the corresponding sharp peak seen for $Y_D^\bullet$ at 3.1 MHz (Figure 7c). A probable interpretation for such a broad exchangeable feature is that the well-ordered hydrogen-bonding interaction involving the D2-His189 proton in $Y_D^\bullet$ is replaced in $Y_Z^\bullet$ by a distribution of hydrogen-bonding distances, producing a range of hyperfine couplings and hydrogen-bonding strengths. The median distance of the exchangeable proton would be around 1.94 Å based on the point dipole approximation used earlier and a spin density of 0.25 on the phenolic oxygen (Tommos et al., 1995). Evidence for the exchangeable proton would not have been observed in the lower resolution cw ENDOR spectra run in H_2O and D_2O of Tommos et al. (1995). Further support for the existence of a disordered hydrogen bond to $Y_Z^\bullet$ comes from deuterium-pulsed ENDOR (Diner et al., 1995; Force et al., 1995) and measurements of the g_x component of the anisotropic **g**-tensor of this radical by using high-field EPR (Un et al., 1996). A likely candidate for the source of the hydrogen bond to $Y_Z^\bullet$ is D1-His190 (Svensson et al., 1990), the D1 homologue of D2-His189 that hydrogen-bonds to $Y_D^\bullet$. Replacement of D1-His190 by site-directed mutation results in a 200-fold slowing in the rate of oxidation of Y_Z under manganese-depleted conditions (Diner et al., 1991; Roffey et al., 1994). This slowing is probably the result of the loss of the immediate acceptor of the phenolic proton that is released along with the electron upon Y_Z oxidation. The distance constraints are probably critical, as only a ~1-Å displacement of the covalently bound proton in $Y_Z(OH)$ to the hydrogen-bonded proton in $Y_Z(O)^\bullet\cdots H$ normally would be required in the movement of the proton donor (tyrosine) to the proton acceptor (base). It is, however, also possible that a water molecule or another residue could be part of a hydrogen-bonded chain between the tyrosyl radical and D1-His190. As in the case of $Y_D^\bullet$, the pK_a of histidine (~6) makes it the most likely proton acceptor, as the pK_a values of water to form the hydronium ion or of an amide bond to its protonated form are much lower, −1.74 and −1, respectively (March, 1968).

Contrasting views, opposing the hydrogen bonding of $Y_Z^\bullet$, have been presented on the basis of room-temperature EPR (Roffey et al., 1994) and FTIR (Bernard et al., 1995) spectra of $Y_Z^\bullet$ in PSII-enriched membranes and core complexes, respectively, isolated from site-directed mutants at D1-His190. The constancy of the EPR line shape of $Y_Z^\bullet$ in D1-His190 mutants is not a strong argument against hydrogen bonding, as the spin-density distributions of $Tyr^\bullet$ in $Y_D^\bullet$ and in ribonucleotide reductase are practically identical (Tommos et al., 1995), despite the fact that the former is hydrogen-bonded and the latter is not. As for FTIR, the assignments of the C−O stretching modes of the spectra observed for $Y_Z^\bullet$ and $Y_D^\bullet$ remain controversial, as does their dependence on hydrogen bonding.

A comparison of the TRIPLE spectra of Figure 7a,c indicates that many of the features of the $Y_Z^\bullet$ spectrum are significantly broadened relative to their $Y_D^\bullet$ homologues. For example, the pair of couplings ((L_dL_d', M_dM_d') observed near 7 MHz in $Y_D^\bullet$ have actually been assigned to the ring 2,6-protons (Hoganson & Babcock, 1992; Rigby et al., 1994; Warncke et al., 1994). These are replaced in $Y_Z^\bullet$ by a single, broad feature at 7.3 MHz (H_zH_z'). Tommos et al. (1995) have used the transient ENDOR technique to examine the β-methylene proton-coupling region (20−40 MHz) for $Y_Z^\bullet$ and have found that these couplings also have broader line widths than those seen in the $Y_D^\bullet$ spectrum. A rotational distribution around the C1−Cβ axis of the tyrosine side chain was invoked in this work to interpret the line width broadening. An alternative view is that a distribution of hydrogen-bond strengths not only is responsible for the broad exchangeable proton feature around 2.7 MHz but also modulates the ring spin densities, broadening all of the ENDOR line widths including the β-methylene proton couplings. This kind of behavior would be consistent with what has been observed for semiquinone radicals (Feher et al., 1985). This latter view, however, is not supported for tyrosyl radicals by deuterium ESEEM of the ring 3,5-protons of $Y_Z^\bullet$ and $Y_D^\bullet$ for the hydrogen-bonded wild-type radical and the non-hydrogen-bonded radical in mutant D2-His189Gln (Tang et al., 1993). In all cases the spectra are identical, indicating that they appear to be insensitive to hydrogen bonding (Warncke et al., 1994; Tommos et al., 1995; K. Warncke and G. Babcock, personal communication). Furthermore, Tommos et al., (1995) argue that a comparison of six tyrosyl radicals from different sources, both hydrogen-bonded and not, reveals that the spin densities at all ring positions differ by no more than 0.01. Part of the broadening of the ring 2,6-protons at 7.3 MHz (H_zH_z') could come from a merging of the inequivalent couplings for the homologous protons observed in $Y_D^\bullet$ (L_dL_d' and M_dM_d'). This is unlikely to be the complete story, however, and the line broadening of the 7.3-MHz feature as well as of E_zE_z', F_zF_z', and G_zG_z' remains unexplained for the moment. Also unexplained for now is the origin of the positive F_zF_z' feature at 3.61 MHz in the difference spectra (Figure 7f,i).

Recently, Mino and Kawamori (1994) reported the ^1H ENDOR spectrum of $Y_Z^\bullet$ from spinach PSII membrane fragments. They concluded that $Y_D^\bullet$ and $Y_Z^\bullet$ have almost identical ^1H ENDOR spectra and similar microenvironments, in contrast to the present data and conclusions using *Synechocystis* 6803. Although we cannot completely exclude the possibility that there is some difference in the $Y_Z^\bullet$ proton hyperfine couplings between cyanobacteria and higher plants,

there are complicating factors in their $Y_Z^•$ spectrum, which was generated and trapped in the presence of $Y_D^•$. Only a fraction of the total tyrosyl radical population was observed, suggesting the possibility that the $Y_D^•$ and $Y_Z^•$ spectra may arise from the same species. In the present study, the $Y_D^•$ radical has been completely eliminated by using a Y_D-less mutant.

Measurement of the rate of loss of $Y_Z^•$ shows a sharp temperature transition (Figure 2), with half of $Y_Z^•$ disappearing upon a 30-s incubation at −20 °C. The primary reductant in this experiment is likely to be ferrocyanide, as the conditions of the experiment (300 μM ferricyanide) and the EPR spectrum of trapped radical favor the absence of Q_A^- accompanying the trapped $Y_Z^•$. Ono and Inoue (1991) have reported that, in PSII membranes depleted of manganese, the A_T band of thermoluminescence, arising from charge recombination between the oxidized donor (proposed to be a histidine radical) and Q_A^-, appears at around −20 °C. The rate of heating (0.5−1 °C/s) and the temperature range over which the emission band appears also imply a 30-s to 1-min lifetime at this temperature. Preliminary measurements (not shown) indicate that the activation energy for the reduction of $Y_Z^•$ by ferrocyanide is close to that measured for charge recombination between $Y_Z^•$ and Q_A^- by Reinman and Mathis (1981), reopening the possibility that the oxidized donor responsible for the A_T thermoluminescence band may be $Y_Z^•$.

The difference in the properties of $Y_Z^•$ and $Y_D^•$ have recently been the object of speculation on what they imply for function, particularly with regard to the interaction between $Y_Z^•$ and the manganese cluster. $Y_Z^•$ has been proposed to act as a hydrogen atom abstractor, removing either sequentially or concertedly an electron and a proton from the water oxidation site (Hoganson et al., 1995; Gilchrist et al., 1995). That the oxidant of Y_Z and the reductant of $Y_Z^•$ are different species, $P680^+$ and the Mn cluster, respectively, might make it necessary to have a mechanism allowing for reorientation of the tyrosine ring to optimize the rates of electron transfer. Such a mechanism would be unnecessary for $Y_D^•$, where the oxidant and reductant are the oxidized and reduced forms of the same redox cofactor, P680. Whether the dispersion in the orientation of the ring would be determined by alternative sources of hydrogen bonds or by alternative conformations imposing different structural constraints on the ring at present is unclear.

Gilchrist et al. (1995) have recently proposed that the manganese cluster may be as close as 4.5 Å to $Y_Z^•$. The presence of bulk solvent molecules close to $Y_Z^•$ would be consistent with the nearby presence of the manganese cluster, which itself requires access to solvent water or its replacement by solvent water in the manganese-depleted core complexes. Furthermore, the presence of only a very small electrogenic phase associated with electron transfer from the manganese cluster to $Y_Z^•$ (Vos et al., 1991) and virtually none associated with proton release from the manganese cluster is consistent with close access to bulk solvent, despite the location of $Y_Z^•$ at the same level within the thylakoid membranes as $Y_D^•$ (Koulougliotis et al., 1995), which is estimated to be 26 Å from the membrane surface (Innes & Brudvig, 1989). The presence of bulk solvent close to Y_Z might also explain in part why the midpoint potential of $Y_Z^•/Y_Z$ is closer to that of $Tyr^•/Tyr$ in aqueous solution (Harriman, 1987) than is $Y_D^•/Y_D$, which is ∼300 mV lower. We expect that, as additional spectroscopic techniques are brought to bare, the ability to trap both redox-active tyrosines of PSII will result in more detailed information on how the protein tunes the redox behavior and protein environments of these redox functional protein residues.

ACKNOWLEDGMENT

We are grateful to Dr. Gerald Babcock for extensive and helpful discussions and to Ms. Mary Jane Reeve for her excellent assistance in isolating the PSII core complexes.

REFERENCES

Babcock, G. T. (1987) in *New Comprehensive Biochemistry: Photosynthesis* (Amesz, J., Ed.) pp 125−158, Elsevier, Amsterdam.
Babcock, G. T., & Sauer, K. (1973) *Biochim. Biophys. Acta 325*, 483−503.
Babcock, G. T., & Sauer, K. (1975) *Biochim. Biophys. Acta 376*, 315−328.
Babcock, G. T., Barry, B. A., Debus, R. J., Hoganson, C. W., Atamian, M., McIntosh, C., Sithole, I., & Yocum, C. F. (1989) *Biochemistry 28*, 9557−9565.
Barry, B. A. (1993) *Photochem. Photobiol. 57*, 179−188.
Barry, B. A., & Babcock, G. T. (1987) *Proc. Natl. Acad. Sci. U.S.A. 84*, 7099−7103.
Barry, B. A., & Babcock, G. T. (1988) *Chem. Scr. A28*, 117−121.
Bernard, M. T., MacDonald, G. M., Nguyen, A. P., Debus, R. J., & Barry, B. A. (1995) *J. Biol. Chem. 270*, 1589−1594.
Boerner, R. J., & Barry, B. A. (1993) *J. Biol. Chem. 268* (23), 17151−17154.
Boerner, R. J., Bixby, K. A., Nguyen, A. P., Noren, G. H., Debus, R. J., & Barry, B. A. (1993) *J. Biol. Chem. 268*, 1817−1823.
Boussac, A., & Etienne, A.-L. (1984) *Biochim. Biophys. Acta 766*, 576−581.
Brettel, K., Schlodder, E., & Witt, H. T. (1984) *Biochim. Biophys. Acta 766*, 403−415.
Buser, C. A., Diner, B. A., & Brudvig, G. W. (1992) *Biochemistry 31*, 29, 8977−8985.
Conjeaud, H., & Mathis, P. (1980) *Biochim. Biophys. Acta 590*, 353−359.
Debus, R. J. (1992) *Biochim. Biophys. Acta 1102*, 269−352.
Debus, R. J., Barry, B. A., Sithole, I., Babcock, G. T., & McIntosh, L. (1988a) *Biochemistry 27*, 9071−9074.
Debus, R. J., Barry, B. A., Babcock, G. T., & McIntosh, L. (1988b) *Proc. Natl. Acad. Sci. U.S.A. 85*, 427−430.
Dekker, J. P., Plijter, J. J., Ouwehand, L., & van Gorkom, H. J. (1984) *Biochim. Biophys. Acta 767*, 176−179.
Diner, B. A., & Babcock, G. T. (1996) Structure, Dynamics, and Energy Conversion Efficiency in Photosystem II, in *Oxygenic Photosynthesis: The Light Reactions* (Ort, D., & Yocum, C., Eds.) Kluwer Academic Publishers, Dordrecht, The Netherlands (in press).
Diner, B. A., Nixon, P. J., & Farchaus, J. W. (1991) *Curr. Opin. Struct. Biol. 1*, 546−554.
Diner, B. A., Tang, X.-S., Zheng, M., Dismukes, G. C., Force, D. A., Randall, D. W., & Britt, R. D. (1995) in *Proceedings of the Tenth International Congress on Photosynthesis* (Mathis, P., Ed.) Kluwer Academic Publishers, Dordrecht, The Netherlands.
Evelo, R. G., Hoff, A. J., Dikanow, S. A., & Tyryshkin, A. M. (1989) *Chem. Phys. Lett. 161*, 479−484.
Feher, G., Isaacson, R. A., Okamura, M. Y., & Lubitz, W. (1985) in *Antennas and Reaction Centers of Photosynthetic Bacteria* (Michel-Beyerle, M. E., Ed.) Chemical Physics 42, pp 174−189, Springer-Verlag, Berlin.
Force, D. A., Randall, D. W., Britt, R. D., Tang, X.-S., & Diner, B. A. (1995) *J. Am. Chem. Soc. 117*, 12643−12644.
Gilchrist, M. L., Ball, J. A., Randall, D. W., & Britt, R. D. (1995) *Proc. Natl. Acad. Sci. U.S.A. 92*, 9545−9549.
Harriman, A. (1987) *J. Phys. Chem. 91*, 6102−6104.
Hoganson, C. W., & Babcock, G. T. (1988) *Biochemistry 27*, 5848−5855.

Hoganson, C. W., & Babcock, G. T. (1992) *Biochemistry 31*, 11874−11880.
Hoganson, C. W., & Babcock, G. T. (1994) Photosystem II, in *Metal Ions in Biological System* (Sigel, H., & Sigel, A., Eds.) Vol. 30, Metalloenzymes Involving Amino Acid Residue and Related Radicals, pp 77−108, Marcel Dekker, Inc., New York.
Hoganson, C. W., Lydakis-Simantiris, N., Tang, X.-S., Tommos, C., Warncke, K., Babcock, G. T., Diner, B. A., McCracken, J., & Styring, S. (1995) *Photosynth. Res.* (in press).
Innes, J. B., & Brudvig, G. W. (1989) *Biochemistry 28*, 1116−1125.
Kirilovsky, D. L., Boussac, A. G. P., van Mieghem, F. J. E., Ducruet, J.-M. R. C., Sétif, P. R., Yu, J., Vermaas, W. F. J., & Rutherford, A. W. (1992) *Biochemistry 31*, 2099−2170.
Kodera, Y., Takura, K., Mino, H., & Kawamori, A. (1992) in *Research in Photosynthesis* (Muratan, N., Ed.) Vol. II, pp 57−60, Kluwer Academic Publishers, Dordrecht, The Netherlands.
Koulougliotis, D., Tang, X.-S., Diner, B. A., & Brudvig, G. W. (1995) *Biochemistry 34*, 2850−2856.
Malkin, R., & Bearden, A. J. (1973) *Proc. Natl. Acad. Sci. U.S.A. 70*, 294−297.
March, J. (1968) in *Advanced Organic Chemistry: Reactions, Mechanisms and Structure*, pp 219−221, McGraw-Hill, New York.
Meier, B. H. (1994) *Adv. Magn. Opt. Reson. 18*, 1−116.
Metz, J. G., Nixon, P. J., Roger, M., Brudvig, G. W., & Diner, B. A. (1989) *Biochemistry 28*, 6960−6969.
Meyer, B., Schlodder, E., Dekker, J. P., & Witt, H. T. (1989) *Biochim. Biophys. Acta 974*, 36−43.
Miller, A.-F., & Brudvig, G. W. (1990) *Biochemistry 29*, 1385−1392.
Mino, H., & Kawamori, A. (1994) *Biochim. Biophys. Acta 1185*, 213−220.
Nugent, J. H. A., Telfer, A., Demetriou, C., & Barber, J. (1990) *FEBS Lett. 255*, 53−58.
Ono, T.-A., & Inoue, Y. (1991) *FEBS Lett. 278*, 183−186.
Rappaport, F., Blanchard-Desce, M., & Lavergne, J. (1994) *Biochim. Biophys. Acta 1184*, 178−192.
Reinman, S., & Mathis, P. (1981) *Biochim. Biophys. Acta 635*, 249−258.
Rigby, S. E. J., Nugent, J. H. A., & O'Malley, P. J. (1994) *Biochemistry 33*, 1734−1742.
Rippka, R., Deruelles, J., Waterbury, J. B., Herdman, M., & Stanier, R. Y. (1979) *J. Gen. Microbiol. 111*, 1−61.
Rodriguez, I. D., Chandrashekar, T. K., & Babcock, G. T. (1987) in *Progress in Photosynthesis Research* (Biggins, J., Ed.) Vol. I, pp 471−473, Martinus Nijhoff Publishers, The Hague, The Netherlands.
Roffey, R. A., van Wijk, K. J., Sayre, R. T., & Styring, S. (1994) *J. Biol. Chem. 269*, 5115−5121.
Rögner, M., Nixon, P. J., & Diner, B. A. (1990) *J. Biol. Chem. 265*, 6189−6196.
Ruffle, S. V., Donnelly, D., Blundell, T., & Nugent, J. H. A. (1992) *Photosynth. Res. 34*, 287−300.
Styring, S., & Rutherford, A. W. (1987) *Biochemistry 26*, 2401−2405.
Svensson, B., Vass, I., Cedergren, E., & Styring, S. (1990) *EMBO J. 9*, 2051−2059.
Svensson, B., Vass, I., & Styring, S. (1991) *Z. Naturforsch. 46c*, 62−73.
Tang, X.-S., & Diner, B. A. (1994) *Biochemistry 33*, 4594−4603.
Tang, X.-S., Chisholm, D. A., Dismukes, G. C., Brudvig, G. W., & Diner, B. A. (1993) *Biochemistry 32*, 13742−13748.
Thompson, L. K., & Brudvig, G. W. (1988) *Biochemistry 27*, 6653−6658.
Tommos, C. A., Davidson, L., Svensson, B., Madsen, C., Vermaas, W. F. J., & Styring, S. (1993) *Biochemistry 32*, 5436−5441.
Tommos, C., Tang, X.-S., Warncke, K., Hoganson, C. W., Styring, S., McCracken, J., Diner, B. A., & Babcock, G. T. (1995) *J. Am. Chem. Soc.* (submitted).
Tso, J., Hunziker, D., & Dismukes, G. C. (1987) *Progress in Photosynthesis Research* (Biggins, J., Ed.) Vol. I, pp 487−490, Martinus-Nijhoff Publ., Dordrecht, The Netherlands.
Un, S., Tang, X.-S., & Diner, B. A. (1996) *Biochemistry* (in press).
van Leeuwen, P. J., Heiman, C., Gast, P., Dekker, J. P., & van Gorkom, H. J. (1993) *Photosynth. Res. 38*, 169−176.
Vass, I., & Styring, S. (1991) *Biochemistry 30*, 830−839.
Vermaas, W. F. J., Rutherford, A. W., & Hansson, O. (1988) *Proc. Natl. Acad. Sci. U.S.A. 85*, 8477−8481.
Vos, M. H., van Gorkom, H. J., & van Leeuwen, P. J. (1991) *Biochim. Biophys. Acta 1056*, 27−39.
Warden, J. T., Blankenship, R. E., & Sauer, K. (1976) *Biochim. Biophys. Acta 423*, 462−478.
Warncke, K., McCracken, J., & Babcock, G. T. (1994) *J. Am. Chem. Soc. 116*, 7332−7340.
Williams, J. G. K. (1988) *Methods Enzymol. 167*, 766−778.
Wu, X., Xie, X., & Wu, X. (1989) *Chem. Phys. Lett. 162*, 325−328.
Yerkes, C. T., & Babcock, G. T. (1980) *Biochim. Biophys. Acta 590*, 360−372.

BI951489P